processes

MDPI

Article

Cost Prediction for Power Transmission and Transformation Projects in High-Altitude Regions Based on a Hybrid Deep-Learning Algorithm

Shasha Peng [1], Ya Zuo [2], Xiangping Li [2], Mingrui Zhao [3] and Bingkang Li [4,*]

[1] Xinjiang Uygur Autonomous Region Development and Reform Commission, Urumqi 830000, China; pengss@163.com
[2] State Grid Xinjiang Electric Power Co., Ltd., Urumqi 830092, China; yazuo@163.com (Y.Z.); xpli2022@126.com (X.L.)
[3] Electric Power Development Research Institute, China Electricity Council (CEC), Beijing 100761, China; mingrui_zhao1990@163.com
[4] Department of Economic Management, North China Electric Power University, Beijing 102206, China
* Correspondence: libingkang@163.com

Abstract

Energy resources are abundant in high-altitude regions, and the construction of power transmission and transformation projects has important value. However, harsh natural environments can increase project costs. To address the issue of insufficient accuracy caused by the impact of extreme weather factors on cost predictions for power transmission and transformation projects in high-altitude regions, this paper first constructs a four-dimensional influencing factor system covering climate and environment, engineering scale, material consumption, and technological economy. On this basis, a hybrid deep-learning model combining an improved whale optimization algorithm (IWOA) and a convolutional neural network (CNN) is then proposed. The model improves the training accuracy of CNNs and avoids falling into local optima through the use of an SGDM optimizer, the L2 regularization method, and the Bayesian optimization method. Nonlinear convergence factors and adaptive weights are introduced to enhance the WOA's ability to optimize the CNN's learning rate. The case analysis results show that, compared with the comparison model, the proposed IWOA-CNN model exhibits a better convergence performance and fitting effect in the training set and a better prediction effect on the test set. Its mean absolute percentage error is as low as 1.51%, which is 10.1% lower than the optimal comparison model. The root mean square error is reduced to 5.07, and the sum of squared errors is reduced by 72.4%, demonstrating high prediction accuracy. The comparative analysis of scenarios further confirms the crucial role of climate environment; that is, the prediction accuracy of models containing a climate dimension is improved by 51.6% compared to models without such a climate dimension, indicating that the nonlinear impact of low temperatures, frozen soil, and other characteristics of high-altitude regions on costs cannot be ignored. The research results of this paper enrich the method system and application scenarios for the cost prediction for power transmission and transformation projects and provide theoretical reference for engineering predictions in other complex geographical environments.

Keywords: high-altitude regions; power transmission and transformation projects; cost prediction; improved whale optimization algorithm; improved convolutional neural network; climate environment

check for updates

Academic Editor: Jean-Louis Dirion

Received: 2 May 2025
Revised: 14 June 2025
Accepted: 29 June 2025
Published: 1 July 2025

Citation: Peng, S.; Zuo, Y.; Li, X.; Zhao, M.; Li, B. Cost Prediction for Power Transmission and Transformation Projects in High-Altitude Regions Based on a Hybrid Deep-Learning Algorithm. *Processes* **2025**, *13*, 2092. https://doi.org/10.3390/pr13072092

Copyright: © 2025 by the authors. Licensee MDPI, Basel, Switzerland. This article is an open access article distributed under the terms and conditions of the Creative Commons Attribution (CC BY) license (https://creativecommons.org/licenses/by/4.0/).

1. Introduction

In recent years, the scale and intensity of power grid transmission project construction have continued to increase, which has led to stricter requirements for project costs [1]. The efficient and accurate prediction of transmission project costs is of great significance for fine control of power grid costs and improvement of infrastructure investment efficiency [2]. Especially in high-altitude regions, the construction of power transmission and transformation projects is of strategic significance and presents a challenge. These regions typically contain abundant mineral, hydro, wind, and solar resources, making them important bases for national energy strategies and key channels for exporting clean energy [3]. China's high-altitude regions cover a vast area, spanning multiple provinces, and the number of related power transmission and transformation projects has been increasing year by year [4]. The construction of such projects is directly related to providing a reliable power supply for millions of people, as well as promoting social stability and economic development in border areas, and the implementation of major energy strategies such as the "Power Transmission From West to East" of the country. The harsh natural environment in high-altitude regions (low temperature, frozen soil, strong winds, snow, etc.) not only greatly increases the technical difficulty of engineering construction but also significantly pushes up its cost [5]. Accurately predicting such costs is of great practical significance for optimizing huge investment decisions, ensuring project economic feasibility, promoting coordinated regional economic development, and achieving efficient development and utilization of energy resources. However, the cost of grid projects is closely related to complex factors such as sample indicator selection, intelligent algorithm performance, and prediction model structure. A large number of uncertain factors make it difficult to accurately predict the cost of grid projects. Therefore, new methods are urgently needed to solve the prediction problem and improve prediction accuracy.

A large number of scholars have conducted research on the influencing factors involved in the cost prediction for power transmission and transformation projects. On the one hand, early research mainly focused on the impact of factors such as human resources and machinery costs; for instance, Ref. [6] analyzed the impact of human transportation on the cost scale and proportion of various parts of power transmission and transformation projects from the perspective of human transportation. Ref. [7] constructed a cost index for power transmission projects, taking into account the dynamic changes in personnel and machine prices, but it did not take into account the impact of construction levels on cost. With the increasing diversity of construction scenarios for power transmission and transformation projects, some scholars have begun to pay attention to the impact of environmental factors or special construction requirements on the cost of power transmission and transformation projects. For example, Ref. [8] correlated geological divisions with transmission engineering quotas and conducted an analysis of the impact of geological divisions on cost. Ref. [9] theoretically analyzed the cost-sensitive factors of overhead transmission projects from the perspectives of wind speed, icing, etc., but did not consider the differences in engineering quantities under different engineering parameters. Ref. [10] examined the impact of environmental investment in power transmission and transformation projects on project cost based on project environmental impact assessment. Ref. [11] provided a detailed analysis of the composition of operation, maintenance, and repair costs for ultra-high voltage equipment, and identified and quantified the factors affecting cost. Ref. [12] conducted a correlation analysis on the cost-influencing factors of ultra-high-voltage transmission lines and screened key indicators that affect cost, but did not conduct in-depth research on the nonlinear relationship between indicators.

For the cost-prediction methods of power transmission and transformation projects, early research mainly used statistical methods for prediction. For example, Ref. [13] used

the ARIMA method to construct a cost-index prediction model for power transmission and transformation projects, and Ref. [14] used decomposition–integration combination prediction and introduced a multiple regression method to predict the cost level of power transmission and transformation projects. This type of method has good applicability in the face of conventional cost prediction for power transmission and transformation projects. However, as the influencing factors on power transmission and transformation project costs become increasingly complex and the application scenarios of power transmission and transformation projects become more diverse, statistical methods gradually show their inapplicability in power transmission and transformation project cost prediction. With the development of computer technology, machine-learning algorithms have gradually been introduced into the field of prediction due to their ability to better fit the complex interrelationships between factors. Relevant scholars have conducted cost predictions for power transmission and transformation projects using machine-learning algorithms. For instance, Ref. [15] used the random forest algorithm to predict small sample engineering cost data and established a high-dimensional small sample engineering cost estimation model. Ref. [16] combined the wolf pack algorithm with an improved least squares support vector product to predict the cost of substation engineering, reducing prediction errors. Refs. [17] and [18], respectively, use an improved ant colony algorithm and an improved NSGA2 algorithm to optimize the cost of power engineering. The backpropagation (BP) neural network, as a widely used machine-learning algorithm, has also received attention in the field of cost prediction for power transmission and transformation engineering. Ref. [19] used a BP neural network for engineering cost prediction, but there were problems involving falling into local minima, resulting in reduced prediction accuracy during prediction. Therefore, relevant scholars have proposed heuristic optimization algorithms for parameter optimization of BP neural network algorithms to improve prediction performance. Ref. [20] used the sparrow search algorithm to optimize the BP neural network model for predicting the cost of substation engineering. Ref. [21] proposed a fault diagnosis method for power transformers based on an improved BP neural network. Ref. [22] applied the particle swarm optimization algorithm (PSO) and BP neural network algorithm to predict residential construction costs, improving the prediction performance of the BP neural network. Ref. [23] used the genetic algorithm BP neural network method to predict engineering costs, which improved the prediction accuracy of the BP neural network.

However, the cost of power transmission and transformation projects is influenced by numerous factors, and there are complex nonlinear relationships among these factors. Traditional machine-learning algorithms often face difficulties in ensuring the goodness of fit when fitting such high-dimensional nonlinear relationships. As a further extension of machine-learning algorithms, deep-learning algorithms have shown better applicability in the field of cost prediction for power transmission and transformation projects. Ref. [24] applied the Levenberg–Marquardt convolutional neural network (LM-CNN) algorithm to identify anomalies in the cost of power transmission and transformation projects, identifying abnormal information and enhancing the ability to monitor and analyze cost data. Ref. [25] applied the LM-CNN algorithm to establish a cost model for power transmission and transformation projects, achieving a balance between prediction accuracy and stability. Ref. [26] used a multi-layer perceptron neural network to predict the cost of public construction projects. Ref. [27] established a construction period prediction model for transmission line engineering based on a Bayesian regression algorithm and a long short-term memory neural network (LSTM) and used modern statistical theory to complete nonlinear modeling, improving prediction efficiency. Ref. [28] combined data mining and a support vector machine algorithm to predict the cost of transmission engineering.

In summary, the existing research on cost prediction for power transmission and transformation projects is relatively rich, presenting diverse research results in identifying influencing factors and cost-prediction methods, providing useful references for this study. However, there is still room for further deepening: Firstly, current research focuses on the analysis of the impact of a single parameter, without considering the construction of a comprehensive index system for the factors affecting the cost of power transmission and transformation projects. Specifically, high-altitude regions are not conducive to the normal construction of power transmission and transformation projects due to their long, low-temperature periods, frequent winds, high wind speeds, and deep permafrost layers [29,30]. In high-altitude regions, the frozen soil area is large and the freezing time is long; it freezes and expands under lower temperatures in winter and melts and settles under rising temperatures in summer. The existence of these frozen soil areas poses great challenges to the construction of power transmission and transformation projects. The high-altitude regions also have adverse conditions such as large interannual temperature differences and large changes in air humidity, and their winter temperatures are lower and last longer [31,32]. Due to their unique low temperatures, frozen soil, and other conditions, the construction costs of power transmission and transformation projects in high-altitude areas are much higher than those in general areas. However, there have been few studies on the cost of power transmission and transformation projects that consider the special conditions of high-altitude areas. Secondly, regarding the handling of overlapping information in the indicator system of influencing factors, existing research has mostly considered linearly reducing the dimensionality of indicators but has not fully considered how to simultaneously handle the problem of overlapping information in linear and nonlinear engineering quantity indicators.

Based on this, this paper focuses on the cost-prediction problem of power transmission and transformation projects in the special scenario of high-altitude regions. Aiming at the nonlinear relationships among multiple influencing factors, a hybrid deep-learning algorithm framework based on cost-prediction technology for power transmission and transformation projects is proposed. Firstly, the influencing factors on the cost of power transmission and transformation projects in high-altitude regions are analyzed, and a targeted set of influencing factors is constructed. On this basis, the improved whale optimization algorithm (WOA) is combined with the improved convolutional neural network (CNN) to optimize the learning rate of the CNN, thereby effectively improving the prediction accuracy. The effectiveness of the proposed model is verified through case analysis. The main contributions of this paper are as follows:

(1) An analysis was conducted on the impact of climate conditions in high-altitude regions on the cost of power transmission and transformation projects, and a factor system for the cost of high-altitude region power transmission and transformation projects was constructed, which includes four dimensions: climate environment, project scale, material consumption, and technical economy. Compared with existing research, the influencing factor system constructed for this paper can better reflect the characteristics of power transmission and transformation projects in high-altitude regions and expand the set of influencing factors for the cost of conventional power transmission and transformation projects.

(2) A hybrid deep-learning algorithm is proposed to predict the cost of power transmission and transformation projects in high-altitude regions by combining the improved WOA and CNN, with the learning rate of CNN as the link. Compared with existing research, the constructed IWOA-CNN algorithm improves the training accuracy of the CNN and avoids falling into local optima through the SGDM optimizer, L2 regularization method, and Bayesian optimization method. By introducing the nonlinear

convergence factor α and adaptive weights, it enhances the ability of the whale algorithm to perform random global and local searches, thereby obtaining the optimal CNN learning rate. Finally, the case analysis verified the effectiveness of the proposed hybrid deep-learning algorithm in the field of cost prediction for power transmission and transformation projects in high-altitude regions.

The remaining chapters of this paper are arranged as follows: Section 2 analyzes the factors affecting the cost of power transmission and transformation projects in high-altitude regions and constructs a system of influencing factors. Section 3 introduces the constructed cost-prediction model for power transmission and transformation projects in high-altitude regions based on hybrid deep-learning algorithms. Section 4 presents the results of the case analysis. Section 5 summarizes this paper.

2. Cost-Influencing-Factors System for Power Transmission and Transformation Projects in High-Altitude Regions

Climate environment is an important consideration factor for the cost of power transmission and transformation projects in high-altitude regions. The extreme low temperatures, heavy snowfall, frequent freeze–thaw cycles, and strong winds in this region have increased the requirements for the material selection, construction techniques, and post-maintenance of power transmission and transformation projects. For example, in low-temperature environments, conventional wires may become fragile and prone to breakage [33], so special low-temperature resistant wires need to be selected, which undoubtedly increases material costs. At the same time, in order to prevent damage to transmission lines caused by snow and ice accumulation, it may be necessary to install de-icing devices or adopt special line designs [34], which will significantly increase the project cost.

The scale of the project plays a crucial role in the cost of power transmission and transformation projects. The length of the line, the capacity of the substation, and the voltage level of the transmission are important parameters that determine the scale of the project. Taking line length as an example, long-distance transmission lines require more towers, conductors, and other auxiliary materials, which not only increases material procurement costs but may also lead to an increase in transportation and installation costs. For example, the increase in substation capacity means the need for larger transformers, switchgear, and more complex control systems, and the high cost of these devices directly affects the overall cost of the project.

The amount of material used directly affects the cost of power transmission and transformation projects in high-altitude regions. Due to the special environment in high-altitude regions, engineering often requires more materials to enhance the stability and durability of the structure. For example, in permafrost regions, in order to ensure the stability of tower foundations, it may be necessary to use a large amount of concrete and steel bars to reinforce the foundation, or to adopt expensive special foundation treatment techniques such as precast piles and deep mixing. Although these measures can improve the quality and safety of the project, they also significantly increase material costs, thereby raising the overall cost of the project.

Technical and economic analysis is an indispensable part of evaluating the cost of power transmission and transformation projects in high-altitude regions. The choice of construction technology not only affects the smooth implementation of the project but also directly impacts the project cost. In high-altitude regions, winter construction techniques and foundation treatment techniques for frozen soil areas may be required [30,35], which often necessitate special equipment and additional construction measures, such as heating equipment and insulation materials, thereby increasing construction costs. At the same time, from the perspective of long-term operation and maintenance, power transmission and transformation projects in

high-altitude regions require more frequent inspections and higher-level maintenance to ensure the stable operation of equipment in harsh environments. These long-term maintenance costs are also an important part of the project cost that cannot be ignored.

Based on the above analysis, this paper constructs a system of influencing factors on the cost of power transmission and transformation projects for high-altitude regions, as shown in Table 1.

Table 1. Factors affecting the cost of power transmission and transformation projects in high-altitude regions.

Dimension	Indicator	Unit	Reference Source
Climate Environment	Annual minimum temperature	°C	Chen et al. [36]
	Annual average wind speed	m/s	Jiang et al. [37]
	Annual maximum snow depth	cm	Guo et al. [38]; Ma et al. [39]
	Depth of frozen soil	cm	Wang et al. [35]; Hjort et al. [40]
	Terrain coefficient	/	Gorman et al. [41]; Wang et al. [42]
Engineering Scale	Number of circuit lines	Number	Kishore and Singal [43]; Reed et al. [44]; Zheng and Mao [45]; Chen et al. [46]; Zhao et al. [47]
	Number of line splits	Number	
	Number of towers	Number	
	Line length	km	
	Transmission and transformation capacity	kVA	
Material Consumption	Wire cross-sectional area	cm^2	Kishore and Singal [43]; Zheng and Mao [45]; Hayati et al. [48]; Yi et al. [49]; Hongyang et al. [50]
	Basic steel	t/km	
	Basic concrete	t/km	
	Basic soil excavation volume	m^3/km	
	Tower steel	t/km	
	Composite insulator	piece/km	
	Number of insulator pieces	piece/km	
	Hanging wire fittings	t/km	
Technical Economy	Operation and maintenance rate	%	Lu et al. [14]; Yang et al. [51]; Wang et al. [52]
	Inflation rate	%	
	Annual average equipment failure rate	%	Lu et al. [14]; Yang et al. [51]; Yang et al. [53]; Yao [54]; Ma et al. [55]; Xiao et al. [56]
	Annual average time to repair faults	Day	
	Equipment scrap rate	%	
	Annual average downtime	h	
	Annual average unplanned power outages	kWh	

3. Model Construction

3.1. Basic Ideas of the Model

The constructed cost-prediction model for power transmission and transformation projects in high-altitude regions is used as follows to determine the nonlinear relationship between project cost F and m influencing factors:

$$F = f(y_1, y_2, \ldots, y_m) \quad (1)$$

Because m indicators are difficult to unify on a unit basis and cannot directly calculate the cost from m indicators, a hybrid deep-learning model is developed to fit the project cost. The relationship expressed by this prediction model is represented by f, and the input–output relationship is shown in Figure 1.

The constructed hybrid deep-learning model consists of two modules: a nonlinear input–output relationship approximation based on a CNN (Module 1) and an optimization of the optimal learning rate of the CNN based on a WOA (Module 2). The core logic of the constructed hybrid model lies in combining the powerful feature extraction and nonlinear

fitting capabilities of a CNN with the global search ability of a WOA to synergistically improve model performance.

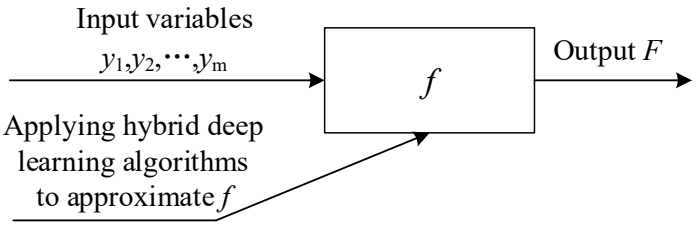


Figure 1. Input–output relationship.

In Module 1, the CNN is designed to directly learn complex nonlinear input–output relationship mappings. In order to effectively train the CNN, the model uses a stochastic gradient descent method (SGDM) with driving factors as the core optimizer. By introducing momentum terms, the SGDM not only considers the direction of the current gradient when updating weight and bias parameters but also accumulates the trend of historical gradients. This significantly accelerates the training process and helps the model smoothly cross flat areas or small valleys of the loss function, thereby improving the stability of parameter updates when randomly selecting small batches of samples for training. In order to further enhance the robustness and generalization ability of the CNN in small samples or noisy data, this module introduces the Bayesian optimization method. Bayesian optimization constructs a probabilistic surrogate model of the objective function (such as validation set error) and intelligently explores and utilizes the hyperparameter space (such as convolution kernel size, number of layers, regularization strength, etc.) based on the acquisition function in order to systematically find the optimal set of hyperparameter configurations. The combination of SGDM and Bayesian optimization effectively alleviates the problems of poor fitting performance and slow convergence caused by poor hyperparameters or gradient oscillations in traditional CNNs during random small batch training.

In Module 2, the WOA is innovatively applied to optimize the crucial hyperparameter in CNN training, namely the learning rate. The model takes the mean absolute percentage error (MAPE) calculated by the CNN on the training/validation set as the target fitness value of the WOA, and sets the learning rate that needs to be optimized as the individual population of the WOA (i.e., each "whale" position represents a candidate learning rate value). The unique advantage of the WOA lies in its search mechanism, which simulates whale predation (bubble-net attack) behavior, with a good balance between global exploration and local development. In order to overcome the drawbacks of slow convergence speed or susceptibility to local optima that may exist in conventional WOAs, this model has made two key improvements to the algorithm itself: firstly, the convergence factor (usually linearly decreasing with iteration) that controls the algorithm from exploration to development has been modified to a non-linear reduction strategy (such as exponential decay), which enables the algorithm to maintain stronger global exploration ability in the initial stage to cover a wider search space and to focus more quickly on potential areas for fine search in the later stage; secondly, the fixed weights used for position updates in the algorithm will be replaced with adaptive weights, which can dynamically adjust based on the current iteration progress or individual fitness, thus endowing the algorithm with more flexible adjustment capabilities in different search stages (global exploration or local development). Through the optimization of the WOA, the model can ultimately automatically find the optimal learning rate for a specific dataset and network structure.

The overall advantage of the IWOA-CNN hybrid architecture is that the WOA's global optimization capability effectively avoids the blindness and time-consuming nature of

manual parameter tuning, and its improvement strategy (nonlinear convergence factor and adaptive weight) significantly improves search efficiency and accuracy; the synergistic effect of Bayesian optimization hyperparameters and the WOA's optimization learning rate ensures that the CNN model can converge quickly and stably while achieving excellent fitting accuracy and generalization performance. Ultimately, a hybrid deep-learning prediction method with high automation, strong robustness, and superior prediction accuracy is constructed.

3.2. Module 1: Nonlinear Relationship Fitting Based on an Improved CNN

(1) Conventional CNN

Figure 2 shows a schematic diagram of the CNN used to predict the cost of power transmission and transformation projects in high-altitude regions. Use the m indicators in Equation (1) to predict the cost F, and sequentially pass through the input layer (with m neurons), the convolution layer (with m convolution kernels, with a size of 3×1), the activation layer (using ReLU function), fully connected layer 1 ($m \times m$ connections), fully connected layer 2 ($m \times m$ connections), and the output layer.

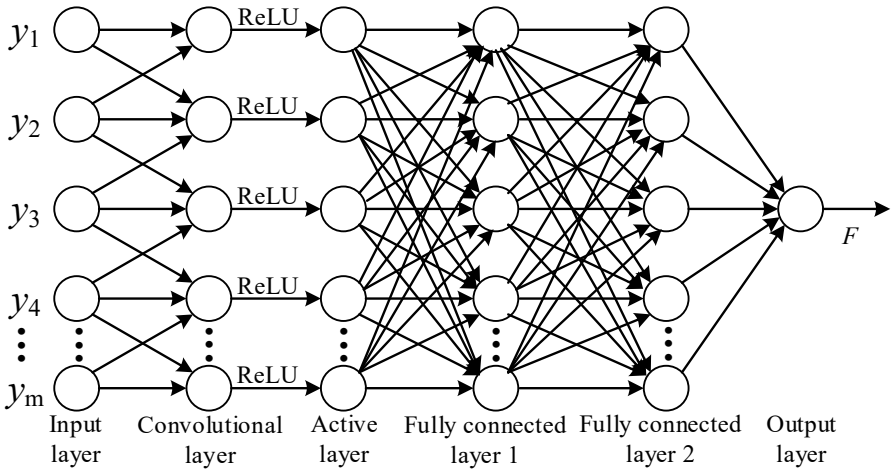


Figure 2. CNN structure.

The formulas for each layer of the CNN are as follows:

(1) Input layer, convolutional layer, and activation layer

Firstly, m indicators are input into the convolutional layer of the convolutional neural network, followed by an activation layer. Equation (2) represents merging the functions of the convolutional layer and the activation layer, that is, performing convolution operations first and then activating. k_2 is the 3×1 convolution kernel, b_2 is the bias, and f_1 represents the output of the ReLU function used for the convolutional layer. Equation (3) explains the ReLU function [57].

$$f_1 = f\left(\sum_{i=1}^{m}(y_i \times k_2) + b_2\right) \tag{2}$$

$$f(c) = \begin{cases} 0, & c < 0 \\ c, & c \geq 0 \end{cases} \tag{3}$$

(2) Two-layer, fully connected layer and output layer

$$f_2 = f(w_3 f_1 + b_3) \tag{4}$$

$$f = f(w_4 f_2 + b_4) \tag{5}$$

Input the output value of the activation layer into the two-layer fully connected layer. In Equation (4), w_3 is the weight of the fully connected layer 1, b_3 is the bias of the fully connected layer 1, $f(\cdot)$ is the activation function, and f_2 is the output of the fully connected layer 1. In Equation (5), w_4 represents the weight of the fully connected layer 2, and b_4 is the bias of the fully connected layer 2.

(2) Improved CNN

The improved CNN adopts the SGDM optimizer, which selects a small batch of samples instead of the entire sample and uses gradient descent to update the weight and bias parameters of the CNN, aiming to solve the problem of poor fitting performance of random small batch samples [58,59]. Introduce the momentum factor when updating weight and bias parameters, subtract the weighted sum of the current and previous iteration gradients to reduce their impact on the weight and bias parameters, and add the L2 regularization term. The relevant formulas are as follows:

$$L_{L2}(\omega, b) = \frac{1}{s}\sum_{k=1}^{s} L\left(f\left(x^{(k)}, \omega, b\right), F^{(k)}\right) + \gamma R_{L2}(\omega) \tag{6}$$

$$g_t^{(1)} = \nabla_\omega L_{L2}(\omega, b) = \frac{1}{s}\sum_{k}^{s} \nabla_\omega L\left(f\left(x^{(k)}, \omega, b\right), F^{(k)}\right) + \gamma \nabla_\omega R_{L2}(\omega) \tag{7}$$

$$m_t^{(1)} = \alpha m_{t-1}^{(1)} - \eta g_t^{(1)} \tag{8}$$

$$\omega_{t+1} = \omega_t + m_t^{(1)} \tag{9}$$

$$g_t^{(2)} = \nabla_b L_{L2}(\omega, b) = \frac{1}{s}\sum_{k}^{s} \nabla_b L\left(f\left(x^{(k)}, \omega, b\right), F^{(k)}\right) \tag{10}$$

$$m_t^{(2)} = \alpha m_{t-1}^{(2)} - \eta g_t^{(2)} \tag{11}$$

$$b_{t+1} = b_t + m_t^{(2)} \tag{12}$$

Equation (6) represents the loss function of the improved CNN with the addition of the L2 regularization term. Firstly, s samples are selected from the training set, including $x^{(1)}, x^{(2)}, \ldots, x^{(s)}$, where $x^{(k)}(k = 1, 2, \ldots, s)$ corresponds to the target of transmission and transformation project cost $F^{(k)}$, and ω and b are the weights and biases of the improved convolutional neural network, respectively. $L_{L2}(\omega, b)$ is the total loss function, $\frac{1}{s}\sum_{k=1}^{s} L\left(f\left(x^{(k)}, \omega, b\right), F^{(k)}\right)$ is the loss function without the regularization term, $\gamma R_{L2}(\omega)$ is the L2 regularization term, and γ is the weight decay coefficient or regularization coefficient.

Equations (7)–(9) show the process of using the SGDM optimizer with L2 regularization to update weights. In Equation (7), $g_t^{(1)}$ is the gradient of weight parameters, t is the number of iterations, and $\nabla_\omega L_{L2}(\omega, b)$ is the gradient of the total loss function with respect to the weight parameters (including L2 regularization); $\frac{1}{s}\sum_{k}^{s} \nabla_\omega L\left(f\left(x^{(k)}, \omega, b\right), F^{(k)}\right)$ represents the gradient of weight parameters for a loss function without regularization terms, and $\gamma \nabla_\omega R_{L2}(\omega)$ represents the gradient of regularization terms with respect to weight parameters. In Equation (8), t is the number of iterations, and $m_t^{(1)}$ is the cumulative momentum of the t-th iteration of the weight parameters; α is the momentum parameter, $m_{t-1}^{(1)}$ is the cumulative momentum of the $t-1$-st iteration of the weight parameter, and η is the learning rate. In Equation (9), ω_{t+1} is the weight parameter for the t + 1th iteration, and ω_t is the weight parameter for the t-th iteration.

Equations (10)–(12) show the process of updating biases using the SGDM optimizer with L2 regularization. L2 regularization is not required for bias, so no L2 regularization term is set in Equation (10). In Equation (10), $g_t^{(2)}$ is the gradient of the bias parameter, t is

the number of iterations, $\nabla_b L_{L2}(\omega, b)$ is the total loss function for the gradient of the bias parameter (excluding L2 regularization), and $\frac{1}{s}\sum_k^s \nabla_b L\left(f\left(x^{(k)}, \omega, b\right), F^{(k)}\right)$ represents the gradient of the loss function without the regularization term for the bias parameter. In Equation (11), $m_t^{(2)}$ is the cumulative momentum of the t-th iteration of the bias parameter, and t is the number of iterations; α is the momentum parameter, and $m_{t-1}^{(2)}$ is the cumulative momentum of the t − 1-st iteration of the bias parameter. In Equation (12), b_{t+1} is the bias parameter for the t + 1th iteration, and b_t is the bias parameter for the t-th iteration.

In order to optimize the hyperparameters in the CNN, a Bayesian optimization method [60] is adopted. The learning rate η varies within the range of [0.01, 1], the momentum of stochastic gradient descent m_t varies within the range of [0.8, 0.98], and the L2 regularization strength varies within the range of [1×10^{-10}, 0.01].

3.3. Module 2: Optimizing CNN Learning Rate Based on Improved WOA

(1) Conventional WOA

The MAPE (P_{MAPE}) obtained by the improved CNN is used as the target fitness value of the WOA, and the learning rate of the improved CNN is used as the population variable of the WOA. This combines the improved CNN with the improved WOA. During the process of updating the fitness value in the WOA, the learning rate of the CNN changes accordingly, thereby altering the prediction accuracy of the CNN.

The fitness index (F_{fit}) is as follows:

$$F_{\text{fit}} = P_{MAPE} = \frac{1}{s}\sum_{k=1}^{s}\left|\frac{\hat{F}^{(k)} - F^{(k)}}{F^{(k)}}\right| \times 100\% \tag{13}$$

In the formula, $\hat{F}^{(k)}$ is the measured value, $F^{(k)}$ is the true value, and s is the number of training samples.

The whale position in the WOA is defined as follows:

$$\eta = X(T) \tag{14}$$

In the formula, $X(T)$ represents the position of the whale. The whale position update in the WOA is an update that improves the learning rate of the CNN.

The WOA treats each whale as a particle and simulates the process of whales surrounding, hunting, and searching for prey. Throughout the process, the whale's position needs to be continuously updated to obtain the global optimal solution.

(2) Improved WOA

The improvement of the WOA involves the addition of convergence factors and adaptive weights for nonlinear algorithms. The description and related formulas for the improved WOA (IWOA) are as follows:

(1) Surrounding process

To complete the encirclement of prey, it is necessary to know the position of the prey and use the current optimal solution as the prey position. Other whales will approach this position, and the position update formula is as follows:

$$X(T+1) = \omega_j X^*(T) - \boldsymbol{A} D_1 \tag{15}$$

$$D_1 = |\boldsymbol{C} X^*(T) - X(T)| \tag{16}$$

$$\boldsymbol{A} = 2a\boldsymbol{r} - a \tag{17}$$

$$\boldsymbol{C} = 2\boldsymbol{r} \tag{18}$$

In the formula, ω_j is the weight of the IWOA, T is the number of iterations, $X^*(T)$ is the optimal solution position at the T-th iteration, D_1 is the distance between the whale individual and the optimal solution position, $\boldsymbol{A}$ and $\boldsymbol{C}$ are coefficient vectors, a is the convergence factor, and $\boldsymbol{r}$ is a random vector with a value range of [0, 1].

For the weight ω_j, changing it from a fixed value to a non-linear cosine function can comply with the setting of global search in the early stage and local search in the later stage. Therefore, the following formula is proposed [61]:

$$\omega_j = -\cos\left(\frac{\pi T}{2T_{\max}} + \pi\right) \tag{19}$$

For the convergence factor a, change the way it linearly decreases and decay it as follows:

$$a = 2 - 0.3 \times \left(\frac{e^{\frac{T}{T_{\max}}} - 1}{e - 1}\right)^{0.6} \tag{20}$$

(2) Predatory process

This type of whale usually uses two methods of predation: bubble-net predation and encirclement predation. When using bubble nets for hunting, the process of updating the position of whales and prey satisfies the logarithmic spiral equation, which is as follows [62]:

$$X(T+1) = D_2 e^{b\prime L}\cos(2\pi L) + \omega_j X^*(T) \tag{21}$$

$$D_2 = \left|X^*(T) - X(T)\right| \tag{22}$$

In the formula, D_2 is the distance between the individual whale and the optimal solution position, b' is the parameter describing the spiral shape, $b' = 1$, and L is a random number.

For bubble-net predation or encirclement predation, the probability P is used as the selection criterion, and the position update equations for the two probabilities are as follows [63]:

$$X(T+1) = \begin{cases} \omega_j X^*(T) - \boldsymbol{A}D_1, & P < 0.5 \\ D_2 e^{b\prime L}\cos(2\pi L) + \omega_j X^*(T), & P \geq 0.5 \end{cases} \tag{23}$$

In the formula, P is the probability distribution of adopting a certain hunting method, with a range of [0, 1]. The above is the update of the position of the whale when the coefficient vector $|\boldsymbol{A}| < 1$. The whale is in the local search stage, and the next whale position is required to be between the current whale position and the prey.

(3) Exploration process

In the case where $|\boldsymbol{A}| \geq 1$, the global search process begins [64]. First, a whale in the population is randomly selected to update its coordinates, and at this point, other particles will move away from the whale to complete the global search process.

$$X(T+1) = X_{\text{rand}} - \boldsymbol{A}D \tag{24}$$

$$D = |\boldsymbol{C}X_{\text{rand}} - X(T)| \tag{25}$$

In the formula, X_{rand} is a randomly selected individual whale, and D is the distance between the whale and a previously randomly selected whale. The final $X(T)$ obtained is the optimal solution of the IWOA, which is the optimal learning rate, and is substituted into the CNN.

In summary, a new cost-prediction model for power transmission and transformation projects in high-altitude regions will be constructed by combining the convergence factor and adaptive weight improved WOA with a Bayesian optimization regularization algo-

rithm and an SGDM optimizer CNN. This model will accelerate convergence and make predictions more accurate.

4. Case Analysis

4.1. Case Setting

The case analysis adopts 75 sets of 10kV overhead line project cost samples provided by a provincial-level power grid enterprise in the high-altitude region of northern China. Fifty sets of samples are used as the training set, and 25 sets of samples are used as the test set. To verify the effectiveness of the prediction method proposed in this paper, four comparative models are set up, with specific parameter settings as follows:

Model 1: IWOA-CNN (model proposed in this paper). The number of whales is 40, and the maximum number of iterations for whales is 100. The SGDM optimizer is used, with 25 inputs and 1 output, a convolution kernel size of 3×1, a total of 25 convolution kernels, and 2 fully connected layers, each with 625 connections. The maximum number of iterations is 3000, and the number of traversal samples is 8. Bayesian optimization method is used for the CNN, with a learning rate variation range of [0.01, 1], a random gradient descent momentum variation range of [0.8, 0.98], and an L2 regularization strength variation range of $[1 \times 10^{-10}, 0.01]$.

Model 2: GA-BP neural network. The network structure is the same as above, with a crossover probability of 0.7 and a mutation probability of 0.1 [65]. The number of training iterations and learning rate are the same as above, and the hidden layer excitation function is tansig [66].

Model 3: Wolf pack algorithm-improved CNN (WPA-CNN). The total number of artificial wolves is 40, the maximum number of iterations is 100, the distance judgment factor is 800 [67], the wolf detection scale factor is 4 [67,68], the maximum number of walks is 30, the step size factor is 1000, the update scale factor is 10 [67,69], the maximum number of walks [70] is 6, and the minimum number of walks is 3. The Adam optimizer is used, with 25 inputs and 1 output, a convolution kernel size of 3×1, a total of 25 convolution kernels, 2 fully connected layers, and 625 connections in each layer.

Model 4: CNN. Using the Adam optimizer, set 25 inputs and 1 output, a convolution kernel size of 3×1, a total of 25 convolution kernels, and the rest are the same as above.

Model 5: PSO-BP. The network structure is 26-6-1, the learning factor is c1 = 2.2, c2 = 0.8; the maximum number of evolutions is 100, and the population size is 40; the initial fitness value is 600, the training times are 50,000, and the learning rate is 0.1. According to Ref. [71], the transfer function from the input layer to the hidden layer is set as a logsig function, the transfer function from the hidden layer to the output layer is a purelin function, and the training function is a traingdm function.

Using MATLAB R2018b as the experimental platform, five representative predictive performance indicators are selected, and their calculation formulas are as follows:

Mean relative error (MRE):

$$P_{MRE} = \frac{1}{n}\sum_{i=1}^{n}\frac{|\hat{y}_i - y_i|}{y_i} \tag{26}$$

Mean absolute percentage error (MAPE):

$$P_{MAPE} = \frac{1}{n}\sum_{i=1}^{n}\left|\frac{\hat{y}_i - y_i}{y_i}\right| \times 100\% \tag{27}$$

Root mean square error (RMSE):

$$P_{RMSE} = \sqrt{\frac{1}{n}\sum_{i=1}^{n}(\hat{y}_i - y_i)^2} \tag{28}$$

Sum of squares error (SSE):

$$P_{SSE} = \sum_{i=1}^{n}(y_i - \hat{y}_i)^2 \tag{29}$$

Mean absolute error (MAE):

$$P_{MAE} = \frac{1}{n}\sum_{i=1}^{n}|\hat{y}_i - y_i| \tag{30}$$

4.2. Analysis of Prediction Results

4.2.1. Convergence Performance

Using the MAPE (P_{MAPE}) as the target fitness value for each model, the convergence of the fitness values for each model is calculated based on the training samples, as shown in Figure 3.

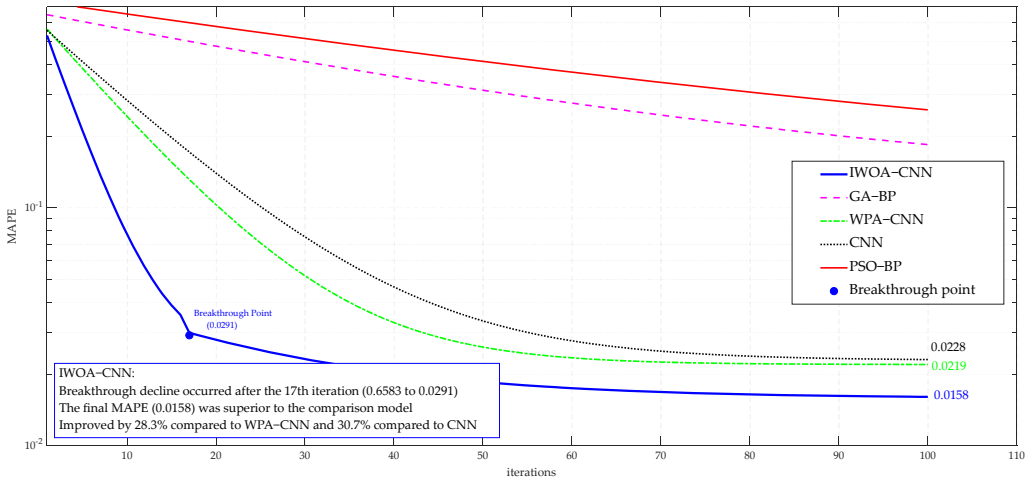


Figure 3. Convergence of the five models.

According to Figure 3, the IWOA-CNN algorithm proposed in this paper demonstrates significant advantages in cost prediction for power transmission and transformation projects in high-altitude regions. From the iterative process, it can be seen that the IWOA-CNN achieved a breakthrough decrease in MAPE value from 0.6583 to 0.0291 in the 17th generation, entering the fine optimization stage about 20 iteration cycles earlier than the comparative algorithms. Its unique WOA mechanism effectively overcomes the low efficiency of traditional CNNs in parameter space search. The final convergence value remains stable at 0.0158, which is 28.3% lower than the optimal comparison model WPA-CNN (0.0219) and 30.7% lower than the CNN (0.0228). In the comparison algorithm, GA-BP and PSO-BP are limited by the local search ability of traditional optimization algorithms, and their convergence speed slows down significantly in the later stage; although the WPA-CNN shows a decreasing competitive trend in the mid-term, the global optimization depth is insufficient. In summary, the IWOA-CNN achieves a balance between fast convergence and high-precision modeling in engineering cost prediction in complex geographical environments by integrating intelligent optimization algorithms and deep-learning collaborative mechanisms. Its steep initial decline

curve and stable final value characteristics can effectively adapt to the nonlinear characteristics of engineering cost data in high-altitude regions.

4.2.2. Fitting Performance

The fitting results of the above five models for 50 training samples are shown in Figure 4.

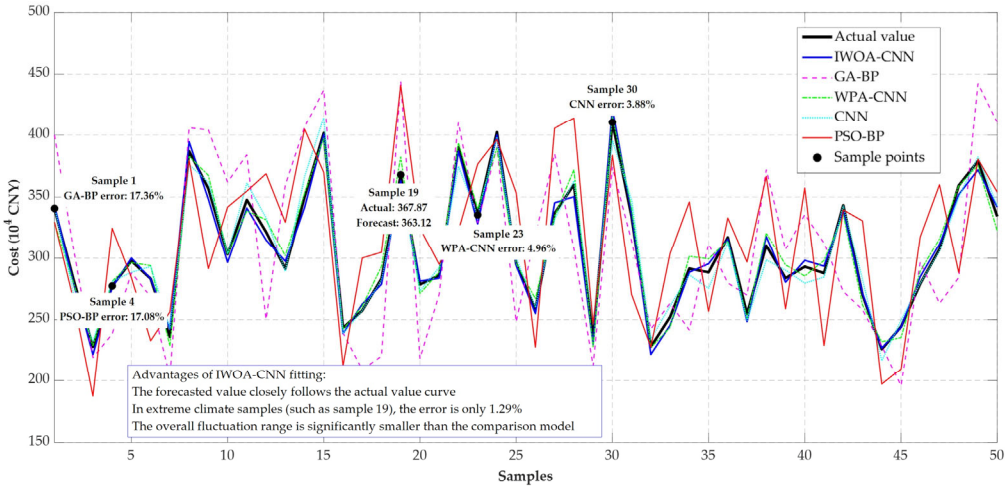


Figure 4. Fitting results of the five models.

Figure 4 shows that the IWOA-CNN model proposed in this paper demonstrates excellent fitting performance in cost predictions for power transmission and transformation projects in high-altitude regions. From the fitting results of 50 training samples, it can be seen that the predicted values of the IWOA-CNN generally closely follow the actual cost curve, and the fluctuation range of its prediction deviation is significantly smaller than that of the comparison model, especially in samples with obvious extreme climate characteristics (such as sample 19, with its actual value of 367.87 and IWOA-CNN prediction of 363.12, an error of only 1.29%), it shows stronger environmental adaptability. The comparative model shows obvious limitations: the GA-BP systematically overestimates in complex terrain samples (such as sample 1, with an error rate of 17.36%), the WPA-CNN has insufficient sensitivity to mutation cost data (such as sample 23, with an error rate of 4.96%), the CNN shows lagging response in time-series fluctuation samples (such as sample 30, with an error rate of 3.88%), while the PSO-BP exhibits prediction instability (sample 4, with an error rate of 17.08%). The IWOA-CNN optimizes the convolution kernel parameters through WOA, achieving high-precision capture of nonlinear features such as frozen soil depth and material transportation costs in high-altitude regions.

4.2.3. Prediction Performance

For the 25 test samples, the prediction results of the five models mentioned above are shown in Figure 5, and the prediction performance of each model is shown in Table 2.

Table 2. Prediction performance of the five models.

Model	P_{MRE}	P_{MAPE}	P_{RMSE}	P_{SSE}	P_{MAE}
IWOA-CNN	0.0151	1.51%	5.0729	643.3652	4.2310
GA-BP	0.1145	11.45%	40.2912	40,584.5114	32.1411
WPA-CNN	0.0168	1.68%	5.4507	742.7602	4.6767
CNN	0.0251	2.51%	8.2384	1696.7611	7.0875
PSO-BP	0.1037	10.37%	34.6873	30,080.1496	29.2890

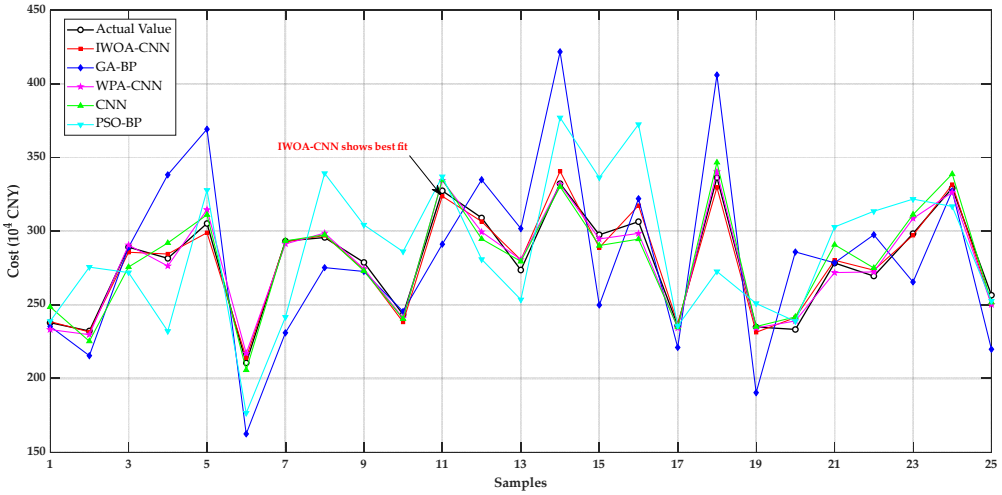


Figure 5. Prediction results of the five models.

The IWOA-CNN model proposed in this paper demonstrates significant predictive advantages on the test set. As shown in Table 2, its MAPE is only 1.51%, which is 10.1% lower than the optimal comparison model WPA-CNN (1.68%) and 39.8% lower than the traditional CNN (2.51%), confirming the effectiveness of the IWOA in parameter tuning. From specific sample observations, the IWOA-CNN performs particularly well in complex working conditions, with a prediction error of only 1.68% for sample 6 (actual value 210.59), while both the GA-BP and PSO-BP produce significant deviations of 22.87% and 16.15%, respectively, exposing the limitations of traditional intelligent algorithms in capturing characteristics of high-altitude frozen soil environments. Although the WPA-CNN performs suboptimally in most samples (such as sample 17, with an error of 0.68%), its RMSE (5.45) still lags behind that of the IWOA-CNN (5.07) by 7.5%, reflecting the accuracy bottleneck of the original CNN in nonlinear regression.

Further analysis of the error distribution shows that the SSE of the IWOA-CNN (643.37) is 13.4% lower than that of the WPA-CNN (742.76), indicating that its prediction results have better stability, especially in high volatility samples (such as sample 14, with an actual value of 332.27 and a prediction error of 2.54%), effectively suppressing outlier interference. The comparative model exhibits significant flaws: the GA-BP falls into local optima due to premature convergence, resulting in a 20.15% overfitting bias in sample 4; the PSO-BP experiences 18.95% directional prediction errors in sample 18 due to the influence of particle swarm inertia mechanism; and the CNN generates a lag response error of 4.3% in sample 23 due to the lack of optimization strategies. The IWOA-CNN successfully achieves accurate modeling of complex engineering factors in high-altitude regions by integrating the global search capability of a WOA with the local feature extraction advantage of a CNN. Its MAE index (4.23) is 85.5% lower than the commonly used PSO-BP (29.29), providing more reliable quantitative support for engineering cost decisions in extreme environments.

4.3. Further Discussion

To further analyze the effectiveness of the cost-prediction system for power transmission and transformation projects in high-altitude regions proposed in this paper, two scenarios are designed:

Scenario 1 (scenario of this paper): The IWOA-CNN algorithm is used for prediction, considering the influencing factors of four dimensions: climate environment, engineering scale, material consumption, and technical economy.

Scenario 2 (comparative scenario): The IWOA-CNN algorithm is used for prediction, and the influencing factors (i.e., climate environment dimensions) reflecting the charac-

teristics of high-altitude regions in Table 1 are removed, only considering the influencing factors of engineering scale, material consumption, and technical economy.

Using the aforementioned 50 sets of samples as the training set and 25 sets of samples as the testing set, the prediction performance of power transmission and transformation projects in the two scenarios is shown in Figure 6 and Table 3.

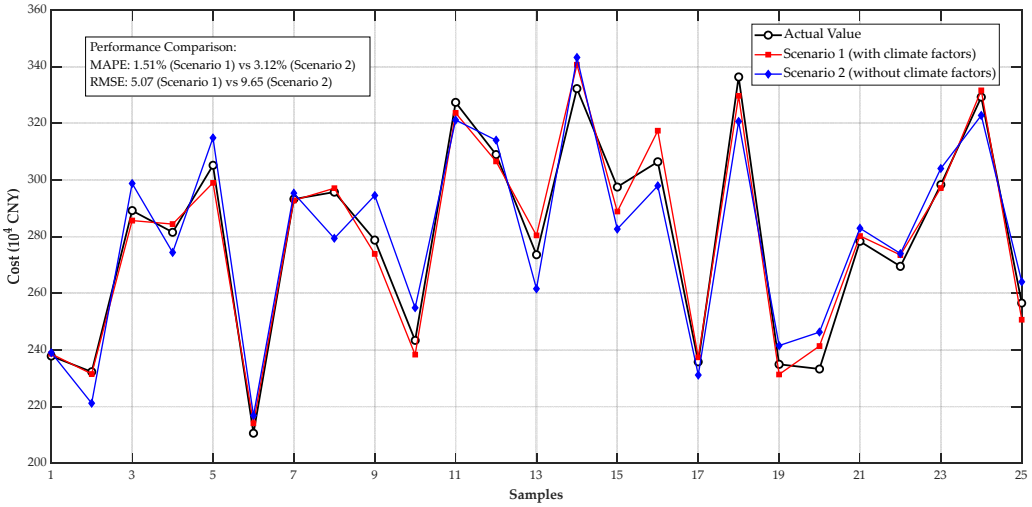


Figure 6. Cost-prediction results for power transmission and transformation projects in two scenarios.

Table 3. Cost-prediction performance for power transmission and transformation projects in two scenarios.

Scenario	P_{MRE}	P_{MAPE}	P_{RMSE}	P_{SSE}	P_{MAE}
Scenario 1	0.0151	1.51%	5.0729	643.3652	4.2310
Scenario 2	0.0312	3.12%	9.6498	2327.9666	8.6826

This verifies the key role of the climate environment in predicting the cost of power transmission and transformation projects in high-altitude regions through scenario comparison. As shown in Table 3, Scenario 1, which includes climate environment factors, has significantly improved prediction accuracy compared to Scenario 2. The MAPE decreases from 3.12% to 1.51%, a decrease of 51.6%, and the RMSE is reduced from 9.65 to 5.07, a decrease of 47.5%. This performance difference is particularly evident in specific samples, such as Scenario 1 in sample 3 (actual value 289.21), with a prediction error of only 1.22%, while Scenario 2, ignoring climate characteristics, has an error rate of 3.31%, indicating that the thermal expansion and contraction effects of wires in low-temperature environments have not been accurately modeled. The predicted value (343.26) of Scenario 2 in sample 14 (actual value 332.27) shows a 71.4% increase in deviation compared to Scenario 1 (340.71), reflecting the estimation bias of structural reinforcement cost caused by the lack of snow depth and frozen soil characteristics.

The inclusion of climate environment factors significantly improves the prediction stability under extreme working conditions. The SSE in Scenario 1 (643.37) decreases by 72.4% compared to Scenario 2 (2327.97), and its advantage is more prominent in typical high-altitude feature samples: the prediction error of Scenario 2 in sample 6 (actual value 210.59) reaches 3.0%, while Scenario 1 is only 1.68%. The difference is due to the underestimation of basic processing costs caused by the lack of consideration for frozen-soil depth; The predicted value (241.53) of Scenario 2 in sample 19 (actual value 234.93) shows a significant increase in deviation compared to Scenario 1 (231.35), indicating that the tower reinforcement demand under strong wind loads has not been effectively cap-

tured. This accuracy difference confirms the strong nonlinear correlation between climate parameters and engineering costs in high-altitude regions. The IWOA-CNN achieves precise quantification of additional costs for special environments (such as premiums for low-temperature-resistant materials and investment in de-icing devices) by integrating characteristics such as temperature and permafrost.

5. Conclusions

With the accelerated construction of power transmission and transformation projects in high-altitude regions, special climatic conditions such as extreme low temperatures, deep permafrost, strong winds, and snow accumulation have significantly increased project costs. However, traditional prediction methods have insufficient accuracy due to neglecting climatic factors. In response to this issue, this paper constructs a four-dimensional influencing factor system covering climate environment, engineering scale, material consumption, and technical economy. Then, a hybrid deep-learning model (IWOA-CNN) is proposed, which combines the IWOA with a CNN. The model optimizes parameter search efficiency through nonlinear convergence factors and adaptive weights and includes Bayesian hyperparameter optimization to improve model robustness. The applicability and effectiveness of the model are verified using actual engineering data.

The results show that the IWOA-CNN is significantly better than traditional models in terms of prediction accuracy and stability. The MAPE of the test set is only 1.51%, which is 10.1% lower than the optimal comparison model (WPA-CNN). The RMSE is reduced to 5.07, and the SSE is reduced by 72.4%. The comparative analysis of scenarios further confirms the key role of climate environment factors: the MAPE reduction of the model with climate dimension (Scenario 1) compared to the model without climate dimension (Scenario 2) is 51.6%, indicating that the nonlinear effects of low temperature, frozen soil, and other features on costs cannot be ignored. Research has confirmed that optimizing the CNN's learning rate through an IWOA can effectively capture complex engineering features such as material performance degradation and increased ground treatment costs in high-altitude regions, providing reliable technical support for cost control in extreme environments.

Overall, this paper enriches the research on cost prediction for power transmission and transformation projects in high-altitude regions by integrating climate factors and deep-learning techniques, providing a scientific basis for engineering investment decision-making and cost management. However, there are still limitations in the research, such as limited data sample size and lack of coverage of multi-voltage-level engineering. Future work can be extended to transmission and transformation projects at higher voltage levels, and dynamic climate models can be introduced to enhance temporal prediction capabilities. Meanwhile, transfer learning frameworks can be explored to address generalization issues in small sample scenarios, thereby further enhancing the applicability of the model in complex geographic environments.

Author Contributions: Conceptualization, S.P. and B.L.; methodology, Y.Z.; software, B.L.; validation, X.L. and M.Z.; formal analysis, S.P.; investigation, B.L.; resources, Y.Z.; data curation, X.L.; writing—original draft preparation, B.L.; writing—review and editing, M.Z.; visualization, S.P.; supervision, Y.Z.; project administration, S.P.; funding acquisition, S.P. All authors have read and agreed to the published version of the manuscript.

Funding: This research received no external funding.

Data Availability Statement: The raw data supporting the conclusions of this article will be made available by the authors on request.

Acknowledgments: During the preparation of this manuscript/study, the author(s) used MATLAB 2018b for the purposes of analysis. The authors have reviewed and edited the output and take full responsibility for the content of this publication.

Conflicts of Interest: Authors Ya Zuo and Xiangping Li were employed by the State Grid Xinjiang Electric Power Co., Ltd. The remaining authors declare that the research was conducted in the absence of any commercial or financial relationships that could be construed as a potential conflict of interest.

References

1. Xu, X. Application research of full process engineering consulting in power grid engineering cost management. *IOP Conf. Ser. Earth Environ. Sci.* **2020**, *565*, 012011. [CrossRef]
2. Davila Delgado, J.M.; Oyedele, L.; Bilal, M.; Ajayi, A.; Akanbi, L.; Akinade, O. Big data analytics system for costing power transmission projects. *J. Constr. Eng. Manag.* **2020**, *146*, 05019017. [CrossRef]
3. Proietti, S.; Sdringola, P.; Castellani, F.; Astolfi, D.; Vuillermoz, E. On the contribution of renewable energies for feeding a high altitude Smart Mini Grid. *Appl. Energy* **2017**, *185*, 1694–1701. [CrossRef]
4. Wei, W.; Wu, X.; Wu, X.; Xi, Q.; Ji, X.; Li, G. Regional study on investment for transmission infrastructure in China based on the State Grid data. *Front. Earth Sci.* **2017**, *11*, 162–183. [CrossRef]
5. Wang, J.; Lin, Q.; Zhao, L.; Xing, J.; Yang, S.; Miao, X. Benefit Analysis of a Power Transmission Project in the East of Inner Mongolia. In Proceedings of the 2022 Asia Power and Electrical Technology Conference (APET), Shanghai, China, 11–13 November 2022; pp. 397–401.
6. Gharaibeh, H.M. Managing the cost of power transmission projects: Lessons learned. *J. Constr. Eng. Manag.* **2013**, *139*, 1063–1067. [CrossRef]
7. Wu, H.; Xiao, F.; Zeng, C.; Zhu, X.; Ke, Y. Research on cost analysis method of power transmission and transformation project based on index theory. In Proceedings of the 2022 2nd International Conference on Electrical Engineering and Control Science (IC2ECS), Nanjing, China, 16–18 December 2022; pp. 174–178.
8. Feng, Z.X.; Zhao, B.B.; He, L.; Fang, C. Research in geological environmental evaluation system of transmission line. *Appl. Mech. Mater.* **2014**, *641*, 1238–1245. [CrossRef]
9. Rossi, A.; Jubayer, C.; Koss, H.; Arriaga, D.; Hangan, H. Combined effects of wind and atmospheric icing on overhead transmission lines. *J. Wind Eng. Ind. Aerodyn.* **2020**, *204*, 104271. [CrossRef]
10. Yu, X.; Yu, M.; Yang, X.; Liu, F. Analysis and research on the influencing factors and influencing mechanism of environmental protection facilities in power transmission and transformation project. In *Energy Revolution and Chemical Research*; CRC Press: Boca Raton, FL, USA, 2022; pp. 93–98.
11. Zhou, H.; Xue, Y.; Liu, Z.; Shen, J.; Yu, M.; Wen, F. Measurement and analysis of impacting factors for operation and maintenance costs in UHV substations. *Electr. Power Constr.* **2018**, *39*, 19–29.
12. Li, J.; Zheng, Y.; Hu, X.; He, Y.; Zhang, Y.; Zhao, J. Research on project cost prediction of ultra-high voltage transmission lines based on RF-HKELM. In Proceedings of the International Conference on Internet of Things and Machine Learning (IoTML 2023), Singapore, 15–17 September 2023; Volume 12937, pp. 184–193.
13. Niu, D.; Hua, F. Research on prediction of transmission and transformation project cost index based on ARIMA and exponential smoothing models. In *Proceedings of the 22nd International Conference on Industrial Engineering and Engineering Management 2015: Innovation and Practice in Industrial Engineering and Management (Volume 2)*; Atlantis Press: Paris, France, 2016; pp. 771–779.
14. Lu, Y.; Niu, D.; Qiu, J.; Liu, W. Prediction technology of power transmission and transformation project cost based on the decomposition-integration. *Math. Probl. Eng.* **2015**, *2015*, 651878. [CrossRef]
15. Lai, Q.; Yang, Z.; Jiang, Y. Cost Analysis of power engineering based on improved random forest algorithm. In Proceedings of the 2024 International Conference on Power, Electrical Engineering, Electronics and Control (PEEEC), Athens, Greece, 14–16 August 2024; pp. 1172–1177.
16. Wang, H.; Liang, Y.; Ding, W.; Niu, D.; Li, S.; Wang, F.; Hong, W.-C. The improved least square support vector machine based on wolf pack algorithm and data inconsistency rate for cost prediction of substation projects. *Math. Probl. Eng.* **2020**, *2020*, 6663006. [CrossRef]
17. Kamarposhti, M.A.; Shokouhandeh, H.; Lee, Y.; Kang, S.-K.; Colak, I.; Barhoumi, E.M. Optimizing energy management in microgrids with ant colony optimization: Enhancing reliability and cost efficiency for sustainable energy systems. *Int. J. Low-Carbon Technol.* **2024**, *19*, 2848–2856. [CrossRef]
18. Zou, D.; Ma, L.; Li, C. An enhanced NSGA-II and a fast constraint repairing method for combined heat and power dynamic economic emission dispatch. *Inf. Sci.* **2024**, *678*, 120915. [CrossRef]
19. Wang, B.; Dai, J. Discussion on the prediction of engineering cost based on improved BP neural network algorithm. *J. Intell. Fuzzy Syst.* **2019**, *37*, 6091–6098. [CrossRef]

20. Xu, X.; Peng, L.; Ji, Z.; Zheng, S.; Tian, Z.; Geng, S. Research on substation project cost prediction based on sparrow search algorithm optimized BP neural network. *Sustainability* **2021**, *13*, 13746. [CrossRef]
21. Jin, Y.; Wu, H.; Zheng, J.; Zhang, J.; Liu, Z. Power transformer fault diagnosis based on improved BP neural network. *Electronics* **2023**, *12*, 3526. [CrossRef]
22. Qiao, Y.; Jones, O. Improving Residential construction cost prediction with PSO-BP neural network optimization. *J. Comput. Sci. Softw. Appl.* **2022**, *2*, 6–14.
23. Wu, Y.; Lan, S.; Liu, T. Research on engineering cost prediction based on GA-BP neural network. *Int. J. Bus. Intell. Data Min.* **2025**, *26*, 362–381. [CrossRef]
24. Zhuang, S.; Chen, W.; Zhou, X. Power grid project cost prediction based on improved CNN under low carbon background. *Int. J. Low-Carbon Technol.* **2024**, *19*, 1682–1688. [CrossRef]
25. Wu, X.; Luan, L.; Pan, L.; Li, H. LM-CNN-based automatic cost calculation model for power transmission and transformation projects. *Electr. Power* **2023**, *56*, 157–163.
26. Pessoa, A.; Sousa, G.; Furtado Maués, L.M.; Alvarenga, F.C.; de Gois Santos, D. Cost forecasting of public construction projects using multilayer perceptron artificial neural networks: A case study. *Ing. Investig.* **2021**, *41*, e87737. [CrossRef]
27. Sha, J.; Ye, J.; Yan, H.; Li, J.; Xia, R.; Lu, S. A full process mechanized transmission line engineering duration prediction model based on Bayesian-LSTM. In Proceedings of the 2023 7th International Conference on Electrical, Mechanical and Computer Engineering (ICEMCE), Xi'an, China, 20–22 October 2023; pp. 392–396.
28. Geng, P.; An, L.; Wang, X. Establishment and implementation of power transmission project's cost forecast model based on data mining technology. *Mod. Electron. Tech.* **2018**, *41*, 157–160.
29. Li, P.; Yu, Q.H.; Yan, F.Z.; Huang, Y.S.; Cheng, D.X. Main problems and solutions on design and construction of Qinghai-Tibet DC transmission project in permafrost region. *Appl. Mech. Mater.* **2013**, *353*, 515–523. [CrossRef]
30. Yu, Q.; Ji, Y.; Zhang, Z.; Wen, Z.; Feng, C. Design and research of high voltage transmission lines on the Qinghai–Tibet Plateau—A special issue on the permafrost power lines. *Cold Reg. Sci. Technol.* **2016**, *121*, 179–186. [CrossRef]
31. Kostianaia, E.A.; Kostianoy, A.G. Railway transport adaptation strategies to climate change at high latitudes: A review of experience from Canada, Sweden and China. *Transp. Telecommun.* **2023**, *24*, 180–194. [CrossRef]
32. Wu, X.; Lin, Z.; Niu, F.; Shang, Y.; Fan, X. Cumulative frost heave and hydrothermal process of the high-speed railway subgrade under extreme climate conditions in northwest China. *Transp. Geotech.* **2024**, *48*, 101297. [CrossRef]
33. Cecchi, V.; Knudson, M.; Miu, K. System impacts of temperature-dependent transmission line models. *IEEE Trans. Power Deliv.* **2013**, *28*, 2300–2308. [CrossRef]
34. He, S.; Song, Y.; Huang, H.; He, Y.; Zhou, S.; Gao, Z. Meteorological characteristics of a continuous ice-covered event on ultra-high voltage transmission lines in Yunnan region in 2021. *Atmosphere* **2024**, *15*, 389. [CrossRef]
35. Wang, G.S.; Yu, Q.H.; You, Y.H.; Zhang, Z.; Guo, L.; Wang, S.J.; Yu, Y. Problems and countermeasures in construction of transmission line projects in permafrost regions. *Sci. Cold Arid Reg.* **2014**, *6*, 432–439.
36. Chen, K.; Ou, W.; Zeng, C.; Wu, H.; Ye, M. Research on cost management of power transmission and transformation project based on BIM technology. In Proceedings of the 2024 International Conference on Machine Intelligence and Digital Applications, Ningbo, China, 30–31 May 2024; pp. 141–147.
37. Jiang, Q.; Li, B.; Liu, T. Tech-economic assessment of power transmission options for large-scale offshore wind farms in China. *Processes* **2022**, *10*, 979. [CrossRef]
38. Guo, J.; Li, J.; Rong, C.; Dong, Z.; Guan, W.; Zheng, Y.; Tan, L. Effectiveness evaluation system and evaluation method for anti-ice damage technical transformation project of overhead lines. In Proceedings of the 2019 IEEE 3rd International Electrical and Energy Conference (CIEEC), Beijing, China, 7–9 September 2019; pp. 314–319.
39. Ma, Z.; Zhao, Z.; Liu, C.; Yang, F.; Wang, M. The impacts and adaptation of climate extremes on the power system: Insights from the texas power outage caused by extreme cold wave. *Chin. J. Urban Environ. Stud.* **2022**, *10*, 2250004. [CrossRef]
40. Hjort, J.; Streletskiy, D.; Doré, G.; Wu, Q.; Bjella, K.; Luoto, M. Impacts of permafrost degradation on infrastructure. *Nat. Rev. Earth Environ.* **2022**, *3*, 24–38. [CrossRef]
41. Gorman, W.; Mills, A.; Wiser, R. Improving estimates of transmission capital costs for utility-scale wind and solar projects to inform renewable energy policy. *Energy Policy* **2019**, *135*, 110994. [CrossRef]
42. Wang, L.; Yang, K.; Li, Z.; Wang, W.; Li, X. Intelligent line selection of power transmission and transformation project supported by geographic information technology. In Proceedings of the Ninth International Conference on Mechanical Engineering, Materials, and Automation Technology (MMEAT 2023), Dalian, China, 9–11 June 2023; Volume 12801, pp. 1265–1270.
43. Kishore, T.S.; Singal, S.K. Optimal economic planning of power transmission lines: A review. *Renew. Sustain. Energy Rev.* **2014**, *39*, 949–974. [CrossRef]
44. Reed, L.; Dworkin, M.; Vaishnav, P.; Morgan, M.G. Expanding transmission capacity: Examples of regulatory paths for five alternative strategies. *Electr. J.* **2020**, *33*, 106770. [CrossRef]

45. Zheng, H.; Mao, Y. Prediction of cost of power transmission and transformation project based on neural network. In Proceedings of the 2022 2nd International Signal Processing, Communications and Engineering Management Conference (ISPCEM), Montreal, ON, Canada, 25–27 November 2022; pp. 190–193.
46. Chen, W.; Qi, X.; Fang, J.; Shao, J.; Chen, C. Research on single tower cost prediction technology of transmission line engineering based on 3D design. *J. Phys. Conf. Ser.* **2020**, *1601*, 022035. [CrossRef]
47. Zhao, S.; Chen, H.; Jia, C.; Wang, Y.; Xin, C.; Jiang, X. Comprehensive evaluation and scheme optimization for power transmission and transformation projects with the adoption of carbon reduction technologies. *Energies* **2024**, *17*, 598. [CrossRef]
48. Hayati, D.W.; Chen, J.-H.; Chen, Y.-C.; Li, S.; Machsus, M.; Khoiri, M.; Wang, Q.-C.; Wei, H.-H. Smart cost estimation: Empirical case for extra-high voltage transmission towers. *Heliyon* **2024**, *10*, e31466. [CrossRef] [PubMed]
49. Yi, T.; Zheng, H.; Tian, Y.; Liu, J.-P. Intelligent prediction of transmission line project cost based on least squares support vector machine optimized by particle swarm optimization. *Math. Probl. Eng.* **2018**, *2018*, 5458696. [CrossRef]
50. Zhang, H.; Zhao, Y.; Gao, H.; Wang, N.; Yang, X. Evaluation of technical transformation and transmission project cost and risk control with value at risk. In Proceedings of the 2022 4th International Conference on Electrical Engineering and Control Technologies (CEECT), Shanghai, China, 16–18 December 2022; pp. 1082–1088.
51. Yang, F.; Chen, F.; Zhao, C.; Li, J.; Kang, J. Analysis and prediction of differential operation and maintenance cost of power transmission and transformation. *Procedia Comput. Sci.* **2023**, *228*, 1277–1286. [CrossRef]
52. Wang, Y.; Song, S.; Gao, M.; Wang, J.; Zhu, J.; Tan, Z. Accounting for the life cycle cost of power grid projects by employing a system dynamics technique: A power reform perspective. *Sustainability* **2020**, *12*, 3297. [CrossRef]
53. Yang, H.; Zhang, Z.; Yin, X.; Han, J.; Wang, Y.; Chen, G. A novel short-term maintenance strategy for power transmission and transformation equipment based on risk-cost-analysis. *Energies* **2017**, *10*, 1865. [CrossRef]
54. Yao, F. Cost analysis of power transmission and transformation projects based on the whole life cycle theory. In Proceedings of the 2024 4th International Conference on Computational Modeling, Simulation and Data Analysis, Hangzhou, China, 6–8 December 2024; pp. 352–356.
55. Ma, L.; Wang, Q.; Liao, S.; Guo, T.; Xiong, Y.; Ming, Y.; Zou, Y. Research on cost prediction of power transmission and transformation project based on combination prediction model. *IOP Conf. Ser. Earth Environ. Sci.* **2021**, *769*, 042019. [CrossRef]
56. Xiao, Y.; Gou, R.; Wang, Z.; Wan, Y. Research on the risk-evaluation model of power transmission and transformation projects based on multilevel fuzzy-thought weighting for cloud-model improvement. *Clean Energy* **2022**, *6*, 153–164. [CrossRef]
57. Lin, G.; Shen, W. Research on convolutional neural network based on improved Relu piecewise activation function. *Procedia Comput. Sci.* **2018**, *131*, 977–984. [CrossRef]
58. Liu, Y.; Gao, Y.; Yin, W. An improved analysis of stochastic gradient descent with momentum. *Adv. Neural Inf. Process. Syst.* **2020**, *33*, 18261–18271.
59. Ramezani-Kebrya, A.; Antonakopoulos, K.; Cevher, V.; Khisti, A.; Liang, B. On the generalization of stochastic gradient descent with momentum. *J. Mach. Learn. Res.* **2024**, *25*, 1–56.
60. Sameen, M.I.; Pradhan, B.; Lee, S. Application of convolutional neural networks featuring Bayesian optimization for landslide susceptibility assessment. *Catena* **2020**, *186*, 104249. [CrossRef]
61. Rana, N.; Latiff, M.S.A.; Abdulhamid, S.M.; Chiroma, H. Whale optimization algorithm: A systematic review of contemporary applications, modifications and developments. *Neural Comput. Appl.* **2020**, *32*, 16245–16277. [CrossRef]
62. Sun, W.; Wang, J.; Wei, X. An improved whale optimization algorithm based on different searching paths and perceptual disturbance. *Symmetry* **2018**, *10*, 210. [CrossRef]
63. Huang, Y.; Zhang, L. Improved whale optimization algorithm and its application. *Comput. Eng. Appl.* **2019**, *55*, 220–226+270.
64. Guo, W.; Liu, T.; Dai, F.; Xu, P. An improved whale optimization algorithm for feature selection. *Comput. Mater. Contin.* **2020**, *62*, 337–354. [CrossRef]
65. Han, W.; Nan, L.; Su, M.; Chen, Y.; Li, R.; Zhang, X. Research on the prediction method of centrifugal pump performance based on a double hidden layer BP neural network. *Energies* **2019**, *12*, 2709. [CrossRef]
66. Liang, W.; Wang, G.; Ning, X.; Zhang, J.; Li, Y.; Jiang, C.; Zhang, N. Application of BP neural network to the prediction of coal ash melting characteristic temperature. *Fuel* **2020**, *260*, 116324. [CrossRef]
67. Chen, X.; Cheng, F.; Liu, C.; Cheng, L.; Mao, Y.; Mirjalili, S. An improved wolf pack algorithm for optimization problems: Design and evaluation. *PLoS ONE* **2021**, *16*, e0254239. [CrossRef]
68. Jiang, H.; Yu, Q.; Han, D.; Chen, Y.; Li, Z. A path planning method for unmanned aerial vehicle based on improved wolf pack algorithm. *Concurr. Comput. Pract. Exp.* **2024**, *36*, e8095. [CrossRef]
69. Sun, G.; Zhang, S.; Yang, S.; Zhao, Y. Application of improved wolf pack algorithm in planning and operation of multi-microgrid systems with electric vehicles. *Meas. Sci. Technol.* **2024**, *35*, 096209. [CrossRef]

70. Xu, S.; Li, L.; Zhou, Z.; Mao, Y.; Huang, J. A task allocation strategy of the UAV swarm based on multi-discrete wolf pack algorithm. *Appl. Sci.* **2022**, *12*, 1331. [CrossRef]
71. Lu, Y.; Niu, D.; Li, B.; Yu, M. Cost forecasting model of transmission project based on the PSO-BP method. *TELKOMNIKA (Telecommun. Comput. Electron. Control)* **2014**, *12*, 773–778. [CrossRef]

Disclaimer/Publisher's Note: The statements, opinions and data contained in all publications are solely those of the individual author(s) and contributor(s) and not of MDPI and/or the editor(s). MDPI and/or the editor(s) disclaim responsibility for any injury to people or property resulting from any ideas, methods, instructions or products referred to in the content.